

# Controlled merging and annihilation of localized dissipative structures in an AC-driven damped nonlinear Schrödinger system

Jae K. Jang<sup>1</sup>, Miro Erkintalo<sup>1</sup>, Kathy Luo<sup>1</sup>, Gian-Luca Oppo<sup>2</sup>, Stéphane Coen<sup>1</sup>, and Stuart G. Murdoch<sup>1</sup>

<sup>1</sup>*Dodd-Walls Centre and Department of Physics, The University of Auckland,*

*Private Bag 92019, Auckland 1142, New Zealand, and*

<sup>2</sup>*SUPA and Department of Physics, University of Strathclyde, Glasgow G4 0NG, Scotland*

We report studies of controlled interactions of localized dissipative structures in a system described by the AC-driven damped nonlinear Schrödinger equation. Extensive numerical simulations reveal a diversity of interaction scenarios that are governed by the properties of the system driver. In our experiments, performed with a nonlinear optical Kerr resonator, the phase profile of the driver is used to induce interactions on demand. We observe both merging and annihilation of localized structures, i.e., interactions governed by the dissipative, out-of-equilibrium nature of the system.

Localized structures coexisting with a homogeneous background are ubiquitous phenomena in extended dissipative systems driven far from equilibrium. These structures consist of solitary excitations that manifest themselves as electrical pulses in nerves [1], concentration spots in chemical reactions [2], oscillons in water waves [3, 4] and in granular matter [5], filaments in gas discharges [6], patches and fairy circles in vegetation [7], or feedback and cavity solitons in nonlinear optics [8–10]. More generally, they are referred to as localized dissipative structures (LDSs) or dissipative solitons [11, 12].

Like the conventional solitons of conservative integrable systems, LDSs can interact and collide with each other, sometimes with particle-like characteristics. But while conventional solitons always emerge unscathed from collisions [13], LDSs can form bound states, merge into one, or even annihilate [12]. These complex interactions arise from the non-integrability of nonlinear dissipative systems, and their study is of particular interest to better understand systems outside thermal equilibrium. Merging and annihilation of solitons have been extensively studied experimentally in non-integrable *conservative* systems, mostly with optical waves [14, 15], but also, more recently, with matter waves [16]. In contrast, although several authors have reported complex behaviors of ensembles of LDSs in various settings, experimental observations have been uncontrolled and mostly qualitative (see, e.g., [5, 12]). It is only in gas discharges [17] and in vertically-driven fluids [4] that quantitative measurements of the interaction laws have been obtained, with [4] also resolving the merging dynamics. These two latter examples are realizations of, respectively, a reaction-diffusion system and a parametrically-driven damped nonlinear Schrödinger equation (NLSE) near the 2:1 resonance.

Here we report on a detailed numerical and experimental study of controlled merging and annihilation dynamics of LDSs in a system described by an AC-driven damped NLSE near the 1:1 resonance. Experiments are performed in a nonlinear optical Kerr resonator, in which we can excite LDSs at selected and precise positions, and

systematically induce their interactions. The interactions are triggered by manipulating the phase profile of the driver; the outcome controllably depends on the driving frequency and strength. Two LDSs either merge into one, or are both annihilated. In both cases, we temporally resolve the collision dynamics and clearly observe the dissipative nature of the interaction through analysis of the energy balance.

To better illustrate our experimental findings, we start our discussion by presenting numerical results. In dimensionless form, the AC-driven damped NLSE reads

$$i\Psi_t + |\Psi|^2\Psi + \Psi_{xx} = -i\Psi + iSe^{i\Delta t}. \quad (1)$$

This equation represents in our case the mean-field behavior of a Kerr resonator [18], but is also the small amplitude limit of the AC-driven sine-Gordon equation [19]. It has applications in non-equilibrium systems ranging from plasma physics [20] to Josephson junctions [21], highlighting the general applicability of our study. The equation can be cast into an autonomous form by substituting  $\Psi(x, t) = \psi(x, t)e^{i\Delta t}$ ,

$$i\psi_t + |\psi|^2\psi + \psi_{xx} = -i\psi + \Delta\psi + iS \quad (2)$$

which will be used throughout this Letter.

Depending on the driving strength  $S$  and its frequency  $\Delta$ , Eq. (2) exhibits a range of solutions, which have been extensively investigated [18, 19]. Briefly, the simplest steady-state solutions are homogeneous ( $\psi_x = 0$ ), and they satisfy the well-known cubic steady-state equation  $X = Y^3 - 2\Delta Y + (\Delta^2 + 1)Y$  with  $X = |S|^2$  and  $Y = |\psi|^2$ . The steady-state curve ( $Y$  vs.  $X$ ) is single-valued for  $\Delta < \sqrt{3}$ , whereas for  $\Delta > \sqrt{3}$  it assumes an S-shaped hysteresis cycle with three possible states. The latter range is of more relevance to our experimental configuration [10], and thus the focus of this Letter. Only two of the three states that exist for  $\Delta > \sqrt{3}$  are homogeneously stable (bistability): the negative slope branch is always unstable. For  $Y > 1$ , the upper branch exhibits a Turing-pattern instability (also known as modulation instability) with respect to inhomogeneous perturbations, which can lead to the formation of a stationary periodic

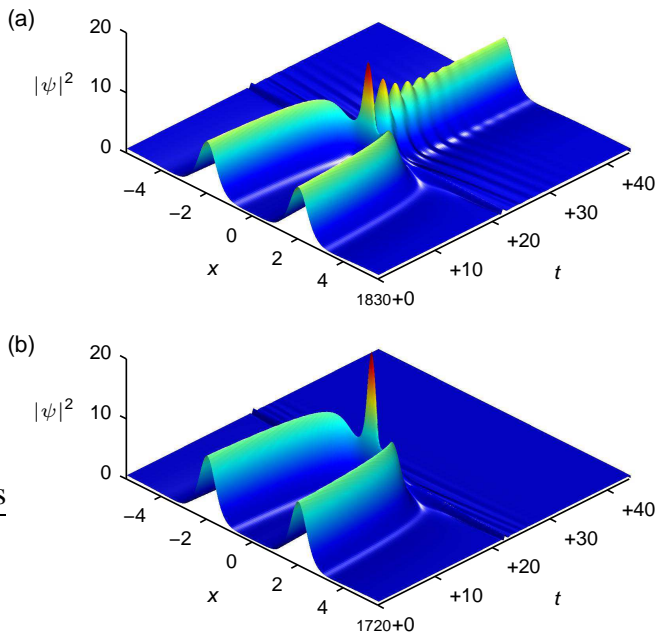


Figure 1. (color online). Numerically simulated dynamics of induced LDS interactions for  $\phi(0) = 0.5$  rad and  $x_0 = 30$ . In (a)  $[\Delta, S_0] = [2.91, 1.87]$  and two LDSs merge into one; in (b)  $[\Delta, S_0] = [3.64, 2.10]$  and two LDSs annihilate one another.

pattern [18]. LDSs can manifest themselves under conditions of coexistence of a patterned solution and a stable homogeneous solution (viz.  $Y < 1$ ). They can be understood to coincide with the patterned solution over a finite region in  $x$ , and with the homogeneous solution elsewhere [22].

We are interested in the dynamics that take place when two LDSs collide. Unlike conservative solitons, widely-separated LDSs of the AC-driven NLSE are phase-locked to the driver, and thus all of them possess identical traits (for given  $X$  and  $\Delta$ ), including frequency ( $\Delta$ ) and velocity. Accordingly, unassisted collisions occur only when two LDSs are sufficiently close to interact attractively [23], yet such interactions are difficult to explore controllably. Inducing collisions by suitably modulating the phase of the driver [24, 25] addresses that issue. Specifically, given  $S(x) = S_0 \exp[i\phi(x)]$ , an LDS at  $x_L$  will move towards the local maximum of  $\phi(x)$  with a drift velocity of  $dx_L/dt = \phi'(x_L)$  [26, 27]. A collision is thus observed when exciting, for example, two LDSs on opposite sides of a local maximum of  $\phi(x)$  [25].

To illustrate such induced collisions, we numerically integrate Eq. (2) using the split-step Fourier method. We assume a Gaussian driver phase profile  $\phi(x) = \phi(0) \exp(-x^2/x_0^2)$ . To create LDSs symmetrically distributed about the phase maximum at  $x = 0$ , we use the initial condition  $\psi(x, 0) = \sqrt{2\Delta} [\text{sech}[\sqrt{\Delta}(x - x_L)] + \text{sech}[\sqrt{\Delta}(x + x_L)]]$ . The initial LDS separation  $2x_L = 70$  is chosen to be much larger than their characteristic

width ( $\sim 1/\Delta$ ) [18, 19, 28] so as to avoid any interactions during the transients leading to the LDS formation. Figures 1(a) and (b) show typical results for two different sets of driver frequency  $\Delta$  and strength  $S_0$ , as listed in the caption, and with  $\phi(0) = 0.5$  rad and  $x_0 = 30$ . These parameters are chosen to replicate our experiments. For clarity, the figures neglect the initial portion of the simulation (which lasts for more than  $t = 1700$ ), during which the two LDSs slowly approach each other from their initial separation of  $2x_L$ . In both cases, it can be seen that the LDSs drift towards each other until they are close enough to interact. The outcome of the collision is, however, markedly different. Indeed, for  $[\Delta, S_0] = [2.91, 1.87]$  the two LDSs merge into one [Fig. 1(a)], whilst for  $[\Delta, S_0] = [3.64, 2.10]$  the intracavity field after the interaction is globally reduced to the homogeneous solution, i.e., the two LDSs annihilate one another [Fig. 1(b)].

It is apparent that the interactions depend on the parameters of the driver. This has been numerically explored further by systematically varying our four control parameters,  $\Delta$ ,  $S_0$ ,  $\phi(0)$ , and  $x_0$ , over a wide range. We have found that  $\Delta$  and  $S_0$  mainly govern the outcome of the collision, while the phase modulation parameters  $\phi(0)$  and  $x_0$  mostly determine the speed at which the LDSs approach each other, i.e., set the timing of the collision. In Fig. 2, we summarize the observed outcome of the interaction as a function of  $S_0$  and  $\Delta$  for the same driver phase modulation  $\phi(x)$  as above. As can be seen, merging (green) and annihilation (blue) occurs in clearly distinct, but adjacent, regions. For a given driving strength  $S_0$ , the system favors annihilation over merging

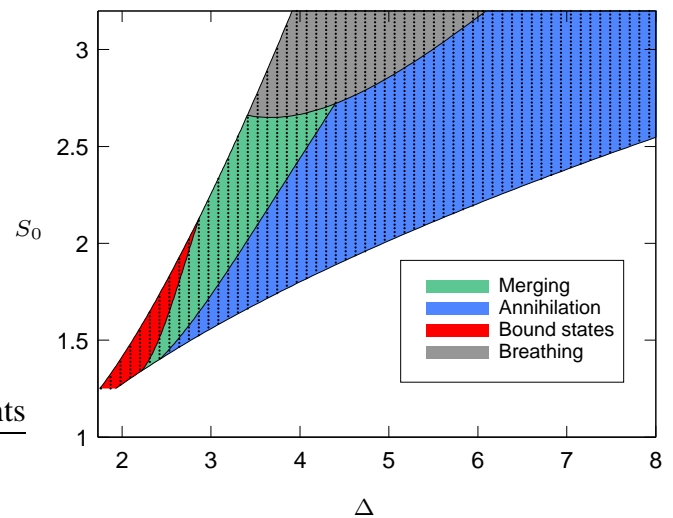


Figure 2. (color online). Results from numerical simulations illustrating the outcome of LDS interactions as a function of driving frequency  $\Delta$  and strength  $S_0$  for  $\phi(0) = 0.5$  rad, and  $x_0 = 30$ . Each solid dot represents a distinct simulation. No LDSs exist in the white-colorcoded area.

at higher driving frequencies. This can be related to the closer proximity to the folding point at  $\Delta_c \sim \pi^2 |S_0|^2 / 8$ , beyond which LDSs cease to exist in this system [19]. Interestingly, in the area marked “bound states” no collision occurs. Instead, the two LDSs form a stable bound state [23, 29]: repulsive interactions of the LDSs resist the drift induced by the driver phase modulation. Not surprisingly, this region slightly grows at the expense of the “merging” region when a shallower phase modulation is used (the merging/annihilation boundary is mostly unaffected). In the grey region, labeled “breathing”, the individual LDSs exhibit breathing as a result of an underlying Hopf bifurcation [19]. Their interaction can lead either to merging or annihilation, depending on the phase of their breathing at the onset of the collision. The bound-state and breather regimes will not be further discussed in this Letter because experimental limitations currently prevent us from observing them.

We now describe our experimental configuration, implemented in the optical domain. Specifically, we induce controllable LDS interactions in a coherently-driven passive optical fiber resonator that exhibits instantaneous Kerr nonlinearity. In the high-finesse limit, this system is known to be governed by Eq. (2), with  $\psi$  representing the slowly-varying envelope of the electric field [18]. The LDSs of such Kerr resonator have been observed experimentally before and are usually referred to as temporal cavity solitons [10]. These are pulses of light that continuously circulate in the resonator, yet remain stationary in a reference frame that is moving at the group velocity of the driving light in the fiber. The transverse coordinate  $x$  in Eq. (2) is thus a “fast-time”  $x \rightarrow \tau$  that is defined in such a reference frame and that allows to describe the temporal profile of the field envelope. In contrast,  $t$  is a “slow-time” that describes changes in the field envelope over consecutive roundtrips around the resonator. The normalization is such that dimensional time-scales  $\tau'$  and  $t'$  (units of s) and the electric field envelope  $E(t', \tau')$  (units of  $W^{1/2}$ ) are related to the dimensionless variables in Eq. (2) by [10]

$$t = \alpha \frac{t'}{t_R}, \quad \tau = \tau' \sqrt{\frac{2\alpha}{|\beta_2|L}}, \quad \psi = E \sqrt{\frac{\gamma L}{\alpha}}. \quad (3)$$

Here  $t_R$  is the roundtrip-time of the resonator,  $\alpha$  is equal to half the percentage of total power loss per round-trip,  $L$  is the resonator length, and  $\beta_2$  ( $< 0$ ) and  $\gamma$  are, respectively, the anomalous group-velocity dispersion and Kerr nonlinearity coefficients of the fiber. The driving strength  $S_0$  is related to the power  $P_{in}$  of the continuous-wave (cw) laser driving the resonator as  $S_0 = (P_{in} \gamma L \theta / \alpha^3)^{1/2}$ , where  $\theta$  is the intensity transmission coefficient of the coupler used to inject the field into the resonator. Finally,  $\Delta$  characterizes the frequency detuning of the cw driving laser at  $\omega$  from the closest resonator resonance at  $\omega_0$ ,  $\Delta \simeq t_R(\omega_0 - \omega) / \alpha$ .

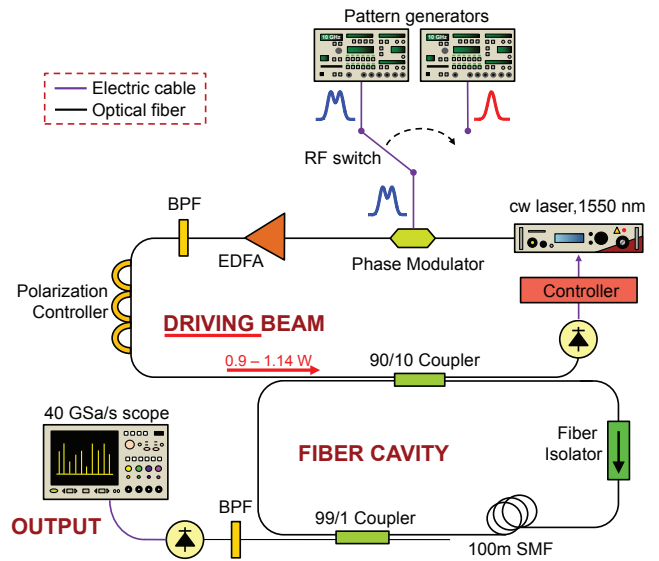


Figure 3. (color online). Experimental setup. cw: continuous-wave, EDFA: erbium-doped fiber amplifier, BPF: band-pass-filter, SMF: single-mode fiber.

A detailed schematic of our experimental setup is shown in Fig. 3. Overall, it is similar to the one used in [27]. As a coherent driver, we use a narrow linewidth cw laser at 1550 nm wavelength, which is amplified up to 1.14 W using an erbium-doped fiber amplifier (EDFA) before being coupled into the resonator by a 90/10 fiber coupler ( $\theta = 0.1$ ). Noise accumulated during the amplification stage is mostly removed with an optical band-pass filter (BPF). The resonator is composed of 100 m of standard silica single-mode fiber (SMF), with  $\beta_2 = -21.4$  ps<sup>2</sup>/km and  $\gamma = 1.2$  W<sup>-1</sup>km<sup>-1</sup>. It also incorporates an optical isolator to prevent resonance of stimulated Brillouin scattering radiation, and a 99/1 fiber coupler through which the intracavity dynamics are monitored with a fast photodiode and a real-time oscilloscope. The overall finesse of the resonator was measured to be  $\mathcal{F} = \pi/\alpha \sim 21.5$ . The BPF at the 1% output filters out the homogeneous cw background that coexists with the LDSs, thereby improving the signal-to-noise ratio of our data [10]. The resonance frequencies of our optical fiber ring generally exhibit fluctuations due to environmental perturbations. To maintain a fixed  $\Delta$ , we therefore actively actuate the driving laser frequency to follow any changes in the resonances, by locking to a set level the optical power reflected off the resonator input [10, 27]. Changing the lock point allows us to controllably adjust  $\Delta$ , but we remark that the accuracy with which we can do so is insufficient to explore the formation of bound states since they manifest themselves over a narrow range of driver frequencies (see Fig. 2). In this context, we also note that, with our current configuration, we are unable to reach power levels required to explore interactions of

breathing LDSs.

To controllably induce LDS interactions, we phase modulate the resonator driving field with a 10 GHz electro-optic modulator. The modulator is driven by one of two 10 GHz programmable pattern generators, selected with an electronic switch. The pattern generators are synchronized to each other by a single external clock, such that the repetition rate of their output patterns is identical to the resonator free-spectral range. The first generator (left in Fig. 3) is configured to produce a pattern of two 130 ps full-width-at-half-maximum electronic pulses with 200 ps separation. These are fed to the phase modulator in the initial stage of the experiment. During that stage, we mechanically perturb the resonator, which results in the direct excitation of two LDSs at the two phase maxima [30]. After the LDSs are stably formed and trapped at the maxima [27], we activate the electronic switch and the phase modulator feed is abruptly changed (within a few nanoseconds) to the output of the second pattern generator. That generator is set to produce a pattern made up of a single pulse whose delay is adjusted to lie halfway between the two pulses generated by the first generator. Accordingly, the LDSs in the resonator find themselves approximately symmetrically positioned about the new single maximum of the phase profile. As in the simulations of Fig. 1, the LDSs thus start drifting towards that maximum, interacting once sufficiently close to each other. Note that the new driver phase profile takes a few photon lifetimes ( $\sim 1 \mu\text{s}$ ) to get imprinted inside the resonator after the switch, but that transient is negligible in regards of the interaction time.

The temporal intensity profile of the intracavity light measured at the 1% output of the resonator is recorded by the oscilloscope (triggered by the pattern generators) as we operate the switch. Successive recordings are vertically concatenated and shown as density plots in Figs. 4(a) and (b), which have been obtained for  $[\Delta, S_0] = [2.91, 1.87]$  and  $[3.64, 2.10]$ , respectively. The first 10 s of the measurements are very similar: two LDSs with 200 ps separation are stably trapped at the maxima of the phase pulses defined by the first pattern generator. After switching to the single phase pulse pattern (which occurs at  $t \simeq 10$  s) and inducing the LDS interaction, a single LDS is seen to remain for  $[\Delta, S_0] = [2.91, 1.87]$  whilst both disappear when  $[\Delta, S_0] = [3.64, 2.10]$ . These results are indicative of merging and annihilation, respectively, which is in agreement with numerical simulations. Indeed, the simulation results in Fig. 1 use the very same parameters as the experiments here. Yet, these results are limited by the slow 1 frame/s acquisition rate of the oscilloscope which does not reveal the transient energy balance dynamics. We have thus also recorded the roundtrip-to-roundtrip evolution of the intracavity energy on the real-time oscilloscope. Experimental results for merging and annihilation are shown as red circles in Figs. 4(c) and (d), respectively, superim-

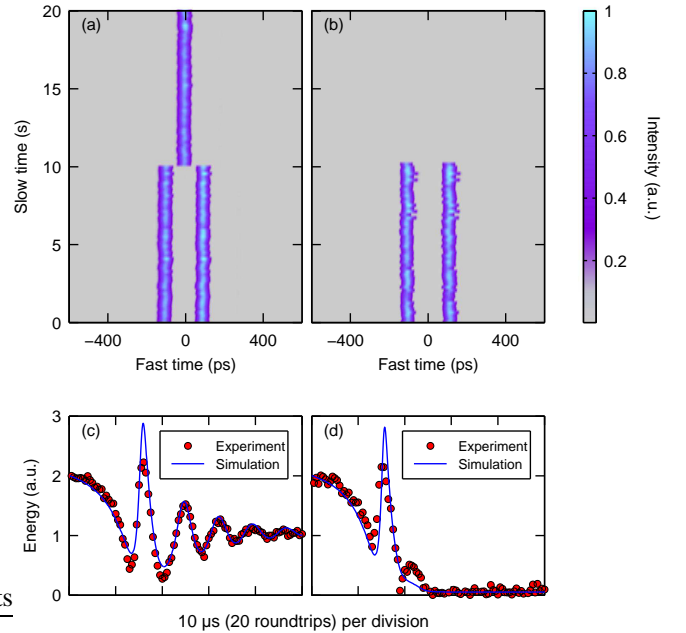


Figure 4. (color online). (a, b) Experimental density plots showing the evolution of the intracavity temporal intensity profile as two LDSs (a) merge into one, and (b) annihilate each other. The successive traces are recorded with a real-time oscilloscope at 1 frame/s. (c, d) The roundtrip-to-roundtrip evolution of the total intracavity energy during LDS (c) merging and (d) annihilation. The experimental data is represented by red circles, and results from numerical simulations are shown as blue solid lines.

posed with results from numerical simulations (blue solid lines). Here we only show the portion of the dynamics corresponding to the final stages of the interaction (the energy stays approximately constant during the slow approach of the two LDSs) and we have normalized the energy such that a single isolated LDS carries the energy 1 a.u. We have also post-processed the numerical simulation results, extracted from data shown in Fig. 1, to take into account the BPF at the resonator output as well as the limited bandwidth of our photodetector. The results in Fig. 4(c, d) clearly confirm that merging and annihilation occur in our experiment and more importantly the dissipative nature of the interactions. For  $[\Delta, S_0] = [2.91, 1.87]$  the energy falls from two to one, implying merging; for  $[\Delta, S_0] = [3.64, 2.10]$  the energy falls from two to zero, implying annihilation.

These results represent, to the best of our knowledge, the first realization of controllable interactions of localized dissipative structures. Our study also provides the first quantitative analysis of such interactions in an AC-driven nonlinear Schrödinger system, and more generally, in any nonlinear dissipative system near the 1:1 resonance. We have numerically identified a diversity of interaction scenarios for different parameters of the system driver. Experiments performed in an optical resonator

show unequivocal evidence of possible selection of LDS interaction by the operator from merging to annihilation.

We acknowledge financial support from the Marsden fund of the Royal Society of New Zealand. M. Erkintalo also acknowledges support from the Finnish cultural foundation.

- 
- [1] A. L. Hodgkin and A. F. Huxley, *J. Physiol.* **117**, 500 (1952).
- [2] J. E. Pearson, *Science* **261**, 189 (1993); K. J. Lee, W. D. McCormick, Q. Ouyang, and H. L. Swinney, *Science* **261**, 192 (1993).
- [3] J. Wu, R. Keolian, and I. Rudnick, *Phys. Rev. Lett.* **52**, 1421 (1984).
- [4] M. G. Clerc, S. Coulibaly, N. Mujica, R. Navarro, and T. Sauma, *Phil. Transact. Royal Soc. A* **367**, 3213 (2009).
- [5] P. B. Umbanhowar, F. Melo, and H. L. Swinney, *Nature* **382**, 793 (1996); O. Lioubashevski, H. Arbell, and J. Fineberg, *Phys. Rev. Lett.* **76**, 3959 (1996).
- [6] Yu. A. Astrov and Yu. A. Logvin, *Phys. Rev. Lett.* **79**, 2983 (1997); Yu. A. Astrov and H.-G. Purwins, *Phys. Lett. A* **283**, 349 (2001).
- [7] O. Lejeune, M. Tlidi, and P. Couteron, *Phys. Rev. E* **66**, 010901 (2002); C. Fernandez-Oto, M. Tlidi, D. Escaff, and M. G. Clerc, *Phil. Transact. Royal Soc. A* **372**, 20140009 (2014).
- [8] V. B. Taranenko, K. Staliunas, and C. O. Weiss, *Phys. Rev. A* **56**, 1582 (1997); B. Schäpers, M. Feldmann, T. Ackemann, and W. Lange, *Phys. Rev. Lett.* **85**, 748 (2000).
- [9] S. Barland, J. R. Tredicce, M. Brambilla, L. A. Lugiato, S. Balle, M. Giudici, T. Maggipinto, L. Spinelli, G. Tissoni, T. Knödl, M. Müller, and R. Jäger, *Nature* **419**, 699 (2002); T. Ackemann, W. J. Firth, and G.-L. Oppo, in *Advances in Atomic, Molecular and Optical Physics*, Vol. 57, edited by E. Arimondo, P. R. Berman, and C. C. Lin (Academic Press, 2009) pp. 323–421.
- [10] F. Leo, S. Coen, P. Kockaert, S.-P. Gorza, Ph. Emplit, and M. Haelterman, *Nature Photon.* **4**, 471 (2010); J. K. Jang, M. Erkintalo, S. G. Murdoch, and S. Coen, *Nature Photon.* **7**, 657 (2013); T. Herr, V. Brasch, J. D. Jost, C. Y. Wang, N. M. Kondratiev, M. L. Gorodetsky, and T. J. Kippenberg, *Nature Photon.* **8**, 145 (2014).
- [11] N. N. Akhmediev and A. Ankiewicz, eds., *Dissipative Solitons: From Optics to Biology and Medicine*, Lecture Notes in Physics, Vol. 751 (Springer, Berlin Heidelberg, 2008).
- [12] H.-G. Purwins, H. U. Bödeker, and Sh. Amiranashvili, *Advances in Physics* **59**, 485 (2010).
- [13] V. E. Zakharov and A. B. Shabat, *Sov. Phys. JETP* **37**, 823 (1973).
- [14] M.-f. Shih, M. Segev, and G. Salamo, *Phys. Rev. Lett.* **78**, 2551 (1997); C. Rotschild, B. Alfassi, O. Cohen, and M. Segev, *Nature Phys.* **2**, 769 (2006).
- [15] V. Tikhonenko, J. Christou, and B. Luther-Davies, *Phys. Rev. Lett.* **76**, 2698 (1996); M.-f. Shih and M. Segev, *Opt. Lett.* **21**, 1538 (1996); W. Królikowski and S. A. Holmstrom, *Opt. Lett.* **22**, 369 (1997); W. Królikowski, B. Luther-Davies, C. Denz, and T. Tschudi, *Opt. Lett.* **23**, 97 (1998).
- [16] J. H. V. Nguyen, P. Dyke, D. Luo, B. A. Malomed, and R. G. Hulet, *Nature Phys.* **10**, 918 (2014).
- [17] H. U. Bödeker, A. W. Liehr, T. D. Frank, R. Friedrich, and H.-G. Purwins, *New J. Phys.* **6**, 62 (2004).
- [18] L. A. Lugiato and R. Lefever, *Phys. Rev. Lett.* **58**, 2209 (1987); M. Haelterman, S. Trillo, and S. Wabnitz, *Opt. Commun.* **91**, 401 (1992); S. Wabnitz, *Opt. Lett.* **18**, 601 (1993).
- [19] I. V. Barashenkov and Yu. S. Smirnov, *Phys. Rev. E* **54**, 5707 (1996); I. V. Barashenkov and E. V. Zemlyanaya, *Physica D* **132**, 363 (1999).
- [20] H. C. Kim, R. L. Stenzel, and A. Y. Wong, *Phys. Rev. Lett.* **33**, 886 (1974).
- [21] A. V. Ustinov, *Physica D* **123**, 315 (1998).
- [22] L. A. Lugiato, *IEEE J. Quantum Elec.* **39**, 193 (2003).
- [23] D. Cai, A. R. Bishop, N. Grønbech-Jensen, and B. A. Malomed, *Phys. Rev. E* **49**, 1677 (1994); M. Brambilla, L. A. Lugiato, and M. Stefani, *Europhys. Lett.* **34**, 109 (1996).
- [24] N. N. Rozanov, *Opt. Spectrosc.* **72**, 243 (1992); N. N. Rosanov, A. V. Fedorov, S. V. Fedorov, and G. V. Khodova, in *Proceedings of SPIE*, Vol. 2039 (SPIE, 1993) pp. 330–341.
- [25] C. McIntyre, A. M. Yao, G.-L. Oppo, F. Prati, and G. Tissoni, *Phys. Rev. A* **81**, 013838 (2010).
- [26] W. J. Firth and A. J. Scroggie, *Phys. Rev. Lett.* **76**, 1623 (1996).
- [27] J. K. Jang, M. Erkintalo, S. Coen, and S. G. Murdoch, arXiv 1410.4836.
- [28] S. Coen and M. Erkintalo, *Opt. Lett.* **38**, 1790 (2013).
- [29] I. V. Barashenkov, Yu. S. Smirnov, and N. V. Alexeeva, *Phys. Rev. E* **57**, 2350 (1998).
- [30] J. K. Jang, M. Erkintalo, S. G. Murdoch, and S. Coen, arXiv 1501.05289.